Distribution of Interstellar Plasma in the Direction of PSR B0525+21 from Data Obtained on a Ground–Space Interferometer

A. S. Andrianov[1]*, T. V. Smirnova[2]**, V. I. Shishov[2]***, C. Gwinn[3]****, and M. V. Popov[1]*****

[1]*Astro Space Center, Lebedev Physical Institute, Russian Academy of Sciences, Moscow, 117997 Russia*

[2]*Pushchino Radio Astronomy Observatory, Astro Space Center, P.N. Lebedev Physical Institute, Pushchino, Russia*

[3]*University of California at Santa Barbara, Santa Barbara, California, USA*

Received September 5, 2016; in final form, December 27, 2016

Abstract—Observations on the RadioAstron ground–space interferometer with the participation of the Green Bank and Arecibo ground telescopes at 1668 MHz have enabled studies of the characteristics of the interstellar plasma in the direction of the pulsar PSR B0525+21. The maximum projected baseline for the ground–space interferometer was 233 600 km. The scintillations in these observations were strong, and the spectrum of inhomogeneties in the interstellar plasma was a power law with index $n = 3.74$, corresponding to a Kolmogorov spectrum. A new method for estimating the size of the scattering disk was applied to estimate the scattering angle (scattering disk radius) in the direction toward PSR B0525+21, $\theta_{\mathrm{scat}} = 0.028 \pm 0.002$ milliarcsecond. The scattering in this direction occurs in a plasma layer located at a distance of $0.1Z$ from the pulsar, where Z is the distance from the pulsar to the observer. For the adopted distance $Z = 1.6$ kpc, the screen is located at a distance of 1.44 kpc from the observer.

1. INTRODUCTION

The dispersion and scattering of radio emission from pulsars on inhomogeneities in the interstellar plasma lead to a whole series of observable effects: angular broadening of the source, stretching of the tail of the pulse profile, and modulation of the emission intensity in time and in frequency (scintillation) on characteristic scales Δt_{sc} and Δf_{dif}. Many observations of pulsar scintillation have been interpreted assuming uniform, isotropic Kolmogorov turbulence [1, 2]. However, there are a many indications that scattering sometimes occurs in discrete, spatially distributed regions (screens) where the plasma has an enhanced electron density. Various observable effects are determined by the spatial distribution of these inhomogeneities. Smirnova et al. [3] demonstrated the presence of two distinct scattering screens in the direction of the pulsar B0950+08, with the scattering occurring primarily in the nearer screen, whose distance from the Earth was 4.4–16.4 pc. The presence of this nearby layer of plasma at a distance of about 10 pc from the observer was first inferred in

studies of the short-time-scale variability of quasars at centimeter wavelengths [4–6]. The time scale for these variations varied with the annual cycle of the Earth in its orbit. The first evidence that the medium responsible for the scintillation of pulsars might be a local medium was obtained in [7, 8] in studies of the scintillation of the nearby pulsars B0950+08 and J0437-47.

Observations with high frequency, time, and spatial resolution using ground and ground–space interferometers can be used to estimate the scattering angles in the directions of pulsars and derive information about the distribution of turbulence in the interstellar plasma along the line of sight. The RadioAstron ground–space interferometer yields the highest angular resolution currently available, to one milliarcsecond (mas) at 324 MHz and 0.2 mas at 1668 MHz. The space radio telescope can operate simultaneously in two frequency ranges, with the two frequency channels receiving radio emission in different polarizations. The high spatial resolution on the ground–space baselines has made it possible to determine not ony the scattering angles in the directions of the pulsars B0329+54 [9], PSR B1641-45, B1749-28, and B1933+16 [10], but also the distances to the corresponding scattering screens.

The aim of our current study was to investigate the parameters of the interstellar plasma in the direction

*E-mail: `andrian@asc.rssi.ru`
**E-mail: `tania@prao.ru`
***E-mail: `shishov@prao.ru`
****E-mail: `cgwinn@physics.ucsb.edu`
*****E-mail: `popov069@asc.rssi.ru`

of the pulsar B0525+21, which has powerful emission at decimeter wavelengths. The pulsar has Galactic latitude and longitude $b = -6.9°$ and $l = 183°.39$, dispersion measure $DM = 50.88$ pc/cm^3, and period $P_1 = 3.745$ s. Interferometric observations of the proper motion of the pulsar have yielded the angular velocities $\mu_\alpha = -20 \pm 19$ mas/yr and $\mu_\delta = -7 \pm 9$ mas/yr [11]. The distance to the pulsar derived using the model of Cordes and Lazio [12] with the indicated disperion measure is $z = 1.6$ kpc.

2. OBSERVATIONS AND PRELIMINARY REDUCTION

B0525+21 was observed on September 18, 2013 at 1668 MHz. The space radio telescope participated in these RadioAstron observations together with ground telescopes at Green Bank, Arecibo, and Kalyazin. The technical and measured parameters of RadioAstron are described in [13]. Unfortunately, the Kalyazin data could not be used due to the presence of strong interference. The Arecibo−RadioAstron baseline had a projected length of 233 600 km, and the Arecibo−Green Bank baseline a projected length of 2553 km. The duration of the observing session was 149 min. The recording was not continuous, and was carried out in scans of 562 s duration (150 periods of the pulsar P_1) with intervals of $10P_1$. The upper and lower subbands were recorded, each with a width of 16 MHz, in two circular polarizations. The data were correlated at the Astro Space Center of the P.N. Lebedev Physical Institute using a pulse window, with dispersion compensation of the signal over the receiver bandwidth. The correlation method is described in [14]. The number of processing channels was chosen so that the frequency resolution was appreciably higher than the expected decorrelation bandwidth at the observing frequency. We used 1024 channels in the 32-MHz bandwidth. The integration window was chosen to be equal to the width of the secondary component of the mean profile at 10% of the maximum level, and was 37.45 ms. A window with this same width outside the pulsed emission was chosen to record the noise. The phase of a pulse was determined from a preliminary analysis of the auto-correlation spectra for the ground telescope. We had complex cross-correlation spectra for all pairs of telescopes at the correlator output, as well as the auto-correlation spectra for each antenna.

3. MAIN THEORETICAL RELATIONS

After passage through the turbulent interstellar plasma, the spectrum of the pulsar radiation can be represented

$$E(\vec{\rho}_1, f, t) = h(f, t)u(\vec{\rho}_1, f, t), \qquad (1)$$

where the modulation factor $u(\vec{\rho}_1, f, t)$ is determined by the interstellar medium, $\vec{\rho}_1$ is the spatial coordinate perpendicular to the line of sight, and $h(f, t)$ is the spectrum of the original pulsar radiation field in the absence of a turbulent medium expressed in terms of frequency f and time t. The measured quantity in interferometric observations is the visiblity function of the quasi-instantaneous response of the interferometer with baseline $\vec{b}$ (the cross-correlation spectrum of the radiation field)

$$I(\vec{\rho}_1, \vec{\rho}_1 + \vec{b}, f, t) \qquad (2)$$
$$= E(\vec{\rho}_1, f, t)E^*(\vec{\rho}_1 + \vec{b}, f, t)$$
$$= H(f, t)j(\vec{\rho}_1, \vec{\rho}_1 + \vec{b}, f, t).$$

Here, $H(f, t) = \langle h(f, t)h^*(f, t)\rangle_h$ (we have adopted $\langle H(f, t)\rangle = 1$), and

$$j(\vec{\rho}_1, \vec{\rho}_1 + \vec{b}, f, t) = u(\vec{\rho}_1, f_1, t_1)u^*(\vec{\rho}_1 + \vec{b}, f, t). \qquad (3)$$

The subscript h denotes averaging over the source statistics. In [15], we determined the correlation function for a ground−space baseline as the modulus of the mean of the second moment

$$J_1(\vec{b}, f) \qquad (4)$$
$$= |\langle I(\vec{\rho}_1, \vec{\rho}_1 + \vec{b}, f, t)I^*(\vec{\rho}_1, \vec{\rho}_1 + \vec{b}, f + \Delta f, t)\rangle|.$$

In the strong scintillation regime [15],

$$J_1(b, f) \qquad (5)$$
$$= |\langle j(\vec{\rho}_1, \vec{\rho}_1 + \vec{b}, f, t)j^*(\vec{\rho}_1, \vec{\rho}_1 + \vec{b}, f + \Delta f, t)\rangle|$$
$$= |B_u(\Delta f)|^2 + |B_u(\vec{b})|^2,$$

where $|B_u(\Delta f)|^2$ is the frequency correlation function for flux fluctuations, which is independent of the baseline, and $B_u(\vec{b})$ is the spatial coherence function of a field with unit mean flux. This is defined as [16]

$$B_u(\vec{b}) = \exp\left[-\frac{1}{2}D_s(\vec{b})\right]. \qquad (6)$$

Here, $D_s(\vec{b})$ is the spatial phase-fluctuation structure function. In the case of a spherical wave,

$$D_s(\vec{b}) = \int_0^Z dz' D_s\left(\frac{z'}{Z}\vec{b}\right). \qquad (7)$$

Here, the integration is carried out from the pulsar ($z' = 0$) to the observer ($z' = Z$). The gradient of the phase structure function D_s is related to the three-dimensional electron-density fluctuation spectrum $\Phi_{N_e}(\vec{q})$. For a power-law turbulence spectrum,

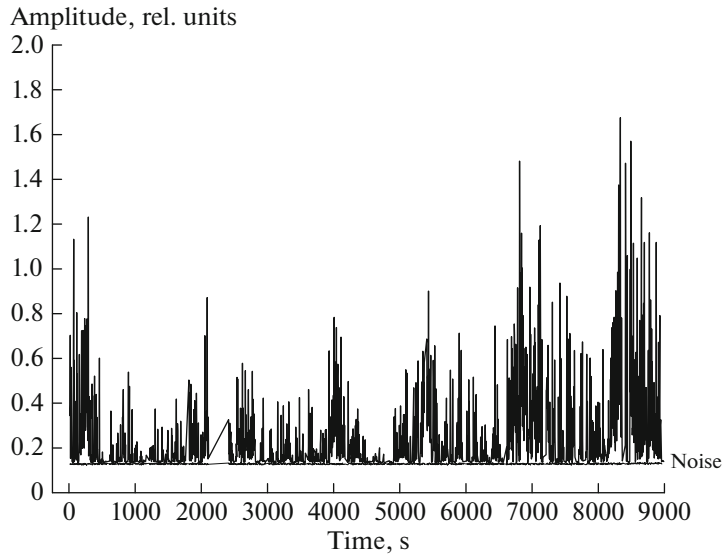$$\Phi_{N_e}(\vec{q}) = C_{N_e}^2|\vec{q}|^{-n}, \qquad (8)$$

Amplitude, rel. units

Fig. 1. Frequency-averaged amplitudes of the pulsar pulses and the noise as a function of time for the Arecibo–Green Bank baseline.
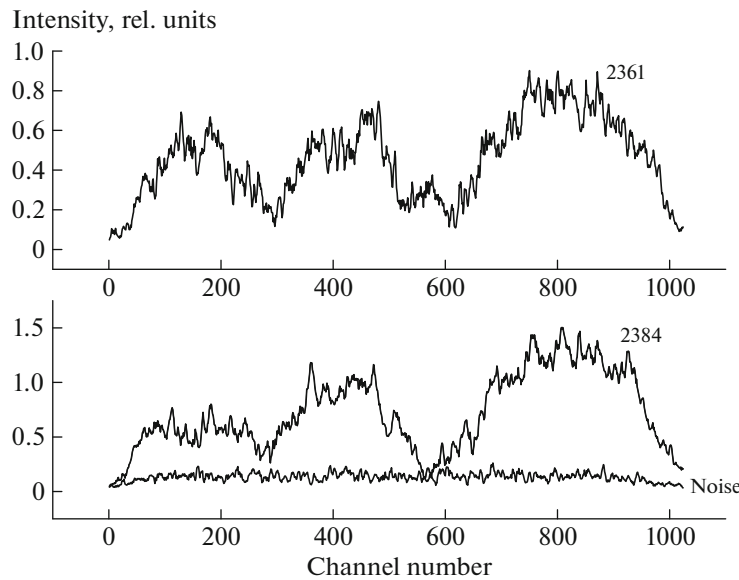
Intensity, rel. units

Fig. 2. Spectra of individual pulses as a function of the channel number for the Arecibo–Green Bank baseline. The numbers indicate the pulse numbers. The frequency resolution was 31.25 kHz, and the time shift between spectra is 86 s.

where the coefficient C_{N_e} characterizes the degree of turbulence and $|\vec{q}|$ is the spatial frequency. The phase-fluctuation structure function also has a power-law form:

$$D_s(\vec{b}) = \left(\frac{|\vec{b}|}{\rho}\right)^{\gamma}, \quad \gamma = n - 2. \quad (9)$$

Here, ρ is the coherence scale of the field in the plane of the observer. We used these relations when analyzing our data.

4. ANALYSIS OF THE DATA

Since the signal was fairly strong, we worked with the individual pulses without time averaging. We obtained the dynamical spectrum of the pulsar, i.e., the variation of the signal intensity in frequency and time, by calculating the modulus of the complex cross-correlation spectra. Figure 1 shows the variation of the modulus of the signal intensity averaged over all frequency channels $\langle |I(t)| \rangle_f$ as a function of time for the Arecibo–Green Bank baseline, together with

the corresponding variations for the noise. Strong variations in the amplitude from pulse to pulse can be seen, which are related to the nature of the pulsar itself. The signal-to-noise ratio reaches 600.

In the correlation processing, the intrinsic variations of the pulsar were suppressed by normalizing the dynamical spectrum $|I(f, t)|$ to $\langle|I(t)|\rangle_f$ for each pulse. Moreover, we applied a correction for the receiver bandwidth, which was obtained by averaging the noise spectra over the entire observing session. Figure 2 presents the unnormalized spectra for individual pulses separated by 23 P_1, or 86 s. It is clear that the frequency structure is preserved with such a time shift. The modulation index obtained from an analysis of the pulse spectra over the entire observing session is $m = 0.8 \pm 0.2$. Here, the uncertainty corresponds to the mean square deviation. For strong scintillations, the modulation index should be unity. Consequently, a strong scintillation regime is realized at 1668 MHz.

To obtain the characteristic scintillation scale in frequency, we determined the normalized frequency auto-covariance function $R_I(\Delta f)$, averaged over the spectra of the individual pulses with amplitudes exceeding $5\sigma_N$ (σ_N is the rms deviation derived from the noise)

$$R_I(\Delta f) \tag{10}$$
$$= \left\langle \frac{\langle|I(f, t)||I(f + \Delta f)|\rangle_f}{[\langle|I(f, t)|\rangle_f]^2} \right\rangle_t.$$

Figure 3 shows $R_I(\Delta f)$ for the Arecibo–Green Bank baseline. The scale Δf_{dif} was determined for the frequency shift at the level of half the amplitude of this function: $\Delta f_{\mathrm{dif}} = 3.9$ MHz. The value of $R_I(\Delta f)$ for zero frequency shift was replaced by an extrapolated value obtained from the values for the neighboring shifts. This was done in order to eliminate the noise component. The noise becomes uncorrelated upon a shift by one channel. The apparent changing in the slope of the function for a shift of 5 MHz is due to the presence of frequency structures that are rare, but broader than the main scale, with widths comparable to the receiver bandwidth. The characteristic scintillation time was determined from the dependence of the covariance function with zero frequency shift on the time shift between pairs of spectra separated by the corresponding time interval, shown in Fig. 4. Here, also, the averaging was carried out over all pairs for which $\langle|I(t)|\rangle_f$ exceeded the threshold indicated above. The shift for which $R_I(\Delta f)$ fell by a factor of $1/e$ was adopted as t_{dif}, and was equal to 160 s.

The frequency–time correlation functions obtained were used in a structure-function analysis of the data. As was shown in [7, 17], analysis of the dependence of the structure function on the

frequency shift can be used to determine which type of scintillation model — diffractive or refractive — is realized in the medium in the direction of the pulsar, and also to determine the index of the power-law spectrum of the density fluctuations associated with inhomogeneities in the interstellar plasma. For small time shifts, the phase structure function (SF) $D_s(\Delta t)$ can be obtained from the covariance function of the intensity fluctuations [17]:

$$D_s(\Delta t) = R_I(\Delta t = 0) - R_I(\Delta t). \tag{11}$$

In the case of a power-law turbulence spectrum, $D_s(\Delta t)$ has the form [17]

$$D_s(\Delta t) = (\Delta t/t_{\mathrm{dif}})^\gamma \quad \text{for } \Delta t \leq t_{\mathrm{dif}}. \tag{12}$$

The following relation is used in the frequency domain:

$$D_s(\Delta f) = R_I(\Delta f = 0) - R_I(\Delta f) \tag{13}$$
$$\text{for } \Delta f \leq \Delta f_{\mathrm{dif}}.$$

In the case of a power-law turbulence spectrum and a diffrative model for the formation of the frequency structure of the scintillations, $D_s(\Delta f)$ has the form [17]

$$D_s(\Delta f) = (\Delta f/\Delta f_{\mathrm{dif}})^{\gamma/2}, \tag{14}$$

where Δt and Δf are the shifts in time and frequency.

Figure 5 presents the temporal (upper) and frequency (lower) structure functions on a double-logarithmic scale. This figure shows that the SFs are power laws when the time and frequency shifts are smaller than the characteristic scales for the inhomogeneities. The slopes of the fitted least-squares lines are $\gamma = 1.74$ for the temporal and $\beta = 0.93$ for the frequency SF. These differ by about a factor of two, testifying that we are dealing with diffractive scintillations. The slopes of the temporal and frequency structure functions should coincide in the case of refractive scintillations [17]. As was shown above, the power-law index for the inhomogeneity spectrum and the slope of the temporal phase SF are related as $n = \gamma + 2$. Consequently, $n = 3.74$, which corresponds to a Kolmogorov inhomogeneity spectrum.

It was shown in [15] that it is possible to measure a small scattering angle in the direction of a pulsar with even a single measurement on a ground and ground–space interferometer, if a non-standard procedure is used to compute the covariance function. The covariance function for a ground–space baseline was determined as the modulus of the mean of the second moment $J_1(\vec{b}, f)$, in accordance with (4). Accordingly, we averaged the real and imaginary parts of the cross-correlation functions of the cross-correlation spectra over the entire observing session and calculated the
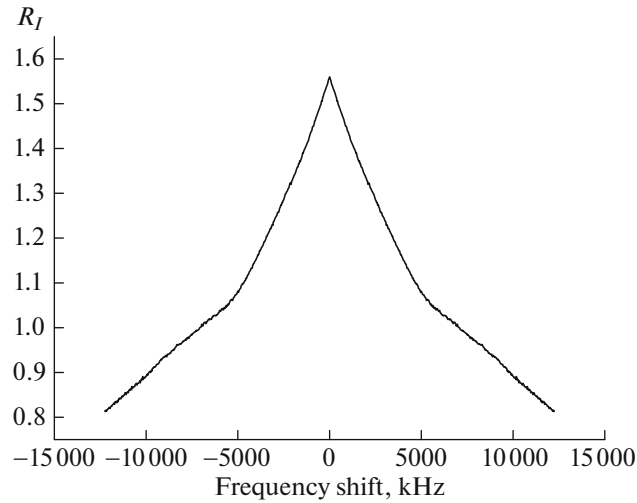
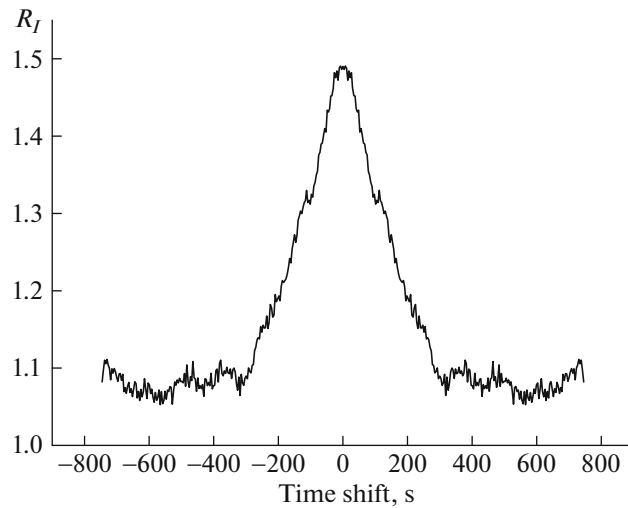**Fig. 3.** Frequency covariance function for the Arecibo−Green Bank baseline.

Fig. 4. Dependence of the cross-correlation coefficient on the time shift between pairs of spectra separated by the corresponding time interval in seconds for the Arecibo−Green Bank baseline.

resulting modulus. Figure 6 presents this function for the Arecibo−RadioAstron baseline. Using (5), the relation $J_1(\vec{b}, f > \Delta f_{\mathrm{dif}})$, and $J_1(\vec{b}, f = 0)$, we obtained for the ground−space interferometer

$$\frac{J_1(\vec{b}, f > \Delta f_{\mathrm{dif}})}{J_1(\vec{b}, \Delta f = 0)} \tag{15}$$

$$= \frac{|B_u(\vec{b})|^2}{[1 + |B_u(\vec{b})|^2]} = 0.23 \pm 0.05$$

or $|B_u(\vec{b})|^2 = 0.30 \pm 0.06$. Here, the uncertainty corresponds to the rms deviation of the amplitude from the mean value in the tail of the covariance function. Using relations (6) and (9) and setting

$\gamma = 1.74$ yields the coherence scale $\rho = (2.1 \pm 0.2) \times 10^5$ km. We obtained the scattering angle (radius of the scattering disk) from the relation $\theta_{\mathrm{scat}} = 1/k\rho = (0.028 \pm 0.002)$ mas at 1668 MHz.

We can obtain information about the distribution of the turublence in the medium along the line of sight from a comparison of ρ and t_{dif}. If the temporal fluctuations are determined by the motion of the pulsar with velocity V, the temporal phase SF is given by

$$D_s(t) = \int_0^Z dz' D\left(\frac{Z - z'}{Z}\vec{V}t\right). \tag{16}$$

Here, $[(Z - z')/Z]\vec{V}t$ is the local spatial scale for

Structure function

$\gamma = 1.74 \pm 0.05$

Time shift, s

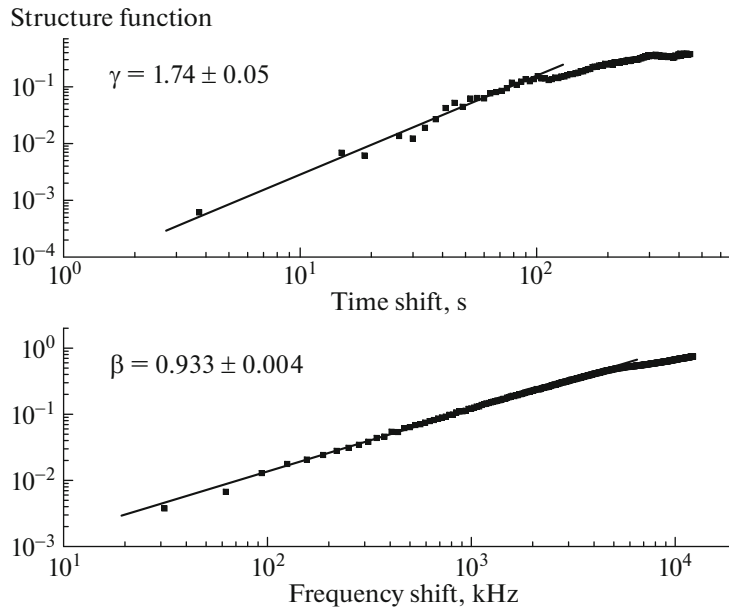$\beta = 0.933 \pm 0.004$

Frequency shift, kHz

Fig. 5. Temporal (upper) and frequency (lower) structure functions, presented on a double-logarithmic scale. The straight lines were derived from least-squares fits to the data obtained for time and frequency shifts whose values were smaller than the characteristic scintillation scales. The indicated uncertainties correspond to those associated with the fitting.
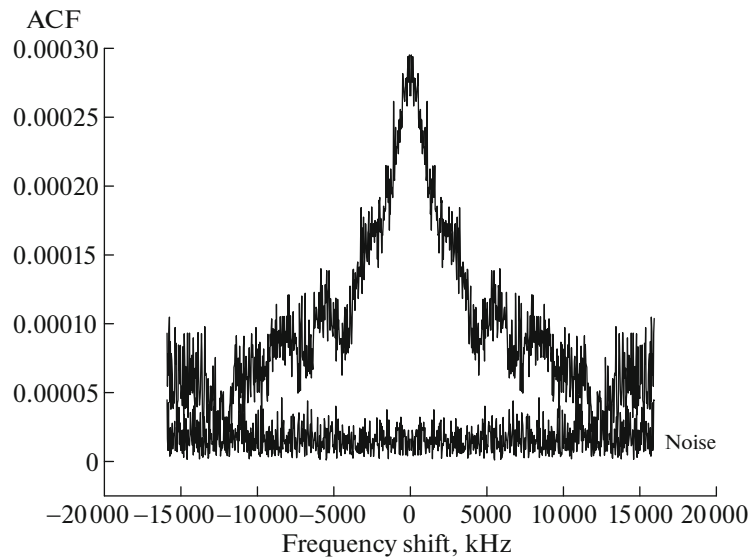
ACF

Noise

Frequency shift, kHz

Fig. 6. Frequency covariance function of the complex cross-correlation spectra for the ground–space baseline Arecibo–RadioAstron, obtained using Eq. (4). The corresponding function calculated for the noise is also shown.

the inhomogeneities responsible for the modulation of the phase. In the case of a statistically uniform turbulence distribution, the scales ρ and $V t_{\mathrm{dif}}$ should be the same. Since the angular velocity of the pulsar is known only with large uncertainty [11], the velocity of the pulsar obtained for a specified distance could also have an uncertainty of 100%. For $Z = 1.6$ kpc,

the pulsar velocity derived from the angular velocity could range from 0–310 km/s. Consequently, even for the maximum velocity, $V t_{\mathrm{dif}} = 49\,600$ km, i.e., at least a factor of 4.5 smaller than the scale ρ. This indicates that the turbulent medium is distributed non-uniformly, and the effective center of gravity of

the turbulent layer is located appreciably closer to the pulsar.

We estimated the position of the center of gravity of the turbulent layer applying a simple model for the distribution of the turbulent medium in the form of a phase screen located at some distance z_1 from the pulsar. Taking the spatial phase-fluctuation SF upon emergence from the phase screen to be $D_{s,s}(b)$, we find that the spatial phase-fluctuation SF in the plane of the observer is

$$D_s(b) = D_{s,s}[(z_1/Z)b]. \quad (17)$$

The temporal phase-fluctuation SF is equal to

$$D_s(t) = D_{s,s}[(Z - z_1)/Z)Vt]. \quad (18)$$

Using a relation from [18], we find for the frequency scale

$$\Delta f_{dif} = G(\gamma)c(kb_s)^2/\pi z_{eff}, \quad (19)$$

where c is the speed of light, k the wave number, $z_{eff} = z_1(Z - z_1)/Z)$ the effective distance to the screen, $b_s = \rho(z_1/Z)$ the coherence scale of the field in the plane of the screen, and G a coefficient, equal to 0.34 for $\gamma = 1.74$ and a thin phase screen. These relations can be used to determine the ratio z_1/Z from the measured values of ρ and Δf_{dif}:

$$\frac{z_1/Z}{1 - z_1/Z} = \pi Z \Delta f_{dif}/[G(\gamma)c(k\rho)^2]. \quad (20)$$

With $\Delta f_{dif} = 3.9$ MHz, $\rho = (2.1 \pm 0.02) \times 10^5$ km, and $Z = 1.6$ kpc, we obtain $z_1/Z = 0.10 \pm 0.02$. Accordingly, the distance from the pulsar to the phase screen is $z_1 = 160$ pc for $Z = 1.6$ kpc. Equating the arguments of $D_s(b)$ and $D_s(t)$ with $t = t_{dif}$ and $b = \rho$ yields the estimated velocity of the pulsar

$$V = (\rho/t_{dif})(z_1/Z)/[1 - (z_1/Z)] \quad (21)$$
$$= (130 \pm 30) \text{ km/s}.$$

This is close to the velocity obtained from interferometric observations yielding a mean proper motion of the pulsar $\mu = 21$ mas/yr for a distance $Z = 1.6$ kpc ($V = 155$ km/s). Although the angular velocity of the proper motion of the pulsar was measured with a large uncertainty, our measurements support a pulsar velocity close to 130 km/s.

5. CONCLUSION

We have succesfully carried out observations of PSR B0525+21 on a ground−space interferometer at 1668 MHz with a baseline of 233 600 km. Our analysis of the temporal and frequency structure functions indicates that the scintillation at this frequency is strong and corresponds to a diffractive model. We have determined the characteristic time

and frequency scales, and shown that the spectrum of the inhomogeneities of the interstellar plasma is a power-law with index $n = 3.74$. We have measured the scattering angle in the direction of PSR B0525+21 to be $\theta_{scat} = 0.028$ mas, and shown that this scattering occurs in a plasma layer located at a distance from the pulsar of $0.1Z$, where $Z = 1.6$ kpc is the distance from the observer to the pulsar.

REFERENCES

1. J. W. Armstrong, B. J. Rickett, and S. R. Spangler, Astrophys. J. **443**, 209 (1995).
2. V. I. Shishov and T. V. Smirnova, Astron. Rep. **469**, 731 (2002).
3. T. V. Smirnova, V. I. Shishov, M. V. Popov, C. R. Gwinn, et al., Astrophys. J. **786**, 115 (2014).
4. L. Kedziora-Chudczer, D. L. Jauncey, M. H. Wieringa, M. A. Walker, G. D. Nicolson, J. E. Reynolds, and A. K. Tzioumis, Astrophys. J. **490**, L9 (1997).
5. J. Dennett-Thorpe and A. G. de Bruyn, Nature **415**, 57 (2002).
6. H. E. Bignall, J. P. Macquart, D. L. Jauncey, J. E. J. Lovell, A. K. Tzioumis, and L. Kedziora-Chudczer, Astrophys. J. **262**, 1050 (2006).
7. T. V. Smirnova, C. R. Gwinn, and V. I. Shishov, Astron. Astrophys. **453**, 601 (2006).
8. T. V. Smirnova and V. I. Shishov, Astron. Rep. **52**, 73 (2008).
9. C. R. Gwinn, M. V. Popov, N. Bartel, A. S. Andrianov, et al., Astrophys. J. **822**, 96 (2016).
10. M. V. Popov, A. S. Andrianov, N. S. Kardashev, A. G. Rudnitskii, T. V. Smirnova, V. A. Soglasnov, E. N. Fadeev, V. I. Shishov, N. Bartel, C. Gwinn, B. C. Joshi, and D. Jauncey, Astron. Rep. **60**, 792 (2016).
11. P. A. Harrison, A. G. Line, and B. Anderson, Mon. Not. R. Astron. Soc. **261**, 113 (1993).
12. J. M. Cordes and T. J. W. Lazio, astro-ph/0207156 (2002).

13. N. S. Kardashev, V. V. Khartov, V. V. Abramov, V. Yu. Avdeev, A. V. Alakoz, Yu. A. Aleksandrov, S. Ananthakrishnan, V. V. Andreyanov, A. S. Andrianov, N. M. Antonov, M. I. Artyukhov, M. Yu. Arkhipov, W. Baan, N. G. Babakin, N. Bartel', et al., Astron. Rep. **57**, 154 (2013).

14. A. S. Andrianov, I. A. Girin, V. E. Zharov, V. I. Kostenko, S. F. Likhachev, and M. V. Shatskaya, Vestn. NPO im. S. A. Lavochkina **3**, 55 (2014).

15. V. I. Shishov, T. V. Smirnova, C. R. Gwinn, A. S. Andrianov, M. V. Popov, A. G. Rudnitskiy, and V. A. Soglasnov, Mon. Not. R. Astron. Soc. (in press).

16. A. M. Prokhorov, F. V. Bunkin, K. S. Gochelashvily, and V. I. Shishov, Proc. IEEE **63**, 790 (1975).

17. V. I. Shishov, T. V. Smirnova, W. Sieber, V. M. Malofeev, V. A. Potapov, D. Stinebring, M. Kramer, A. Jessner, and R. Wielebinski, Astron. Astrophys. **404**, 557 (2003).

18. T. V. Smirnova, V. I. Shishov, and D. R. Stinebring, Astron. Rep. **42**, 766 (1998).

Translated by D. Gabuzda